第 48 卷 第 4 期
2021 年 4 月

湖南大学学报（自然科学版）
Journal of Hunan University（Natural Sciences）

Vol. 48. No. 4.
Apr. 2021

Open Access Article

# Sub-Power Plants Injection to Power Grid Based on Wind and Solar Energy Farms

**A.N. Afandi[1,*], Irham Fadlika[1], Langlang Gumilar[1], Aji P. Wibawa[1], Aripriharta[1], Syaad Patmantara[1], Ilham Aez[1], Eddy Sutadji[2], Tri Kuncoro[3], Marji[2], Yunis Sulistyorini[4], Goro Fujita[5]**

[1] Electrical Engineering, Universitas Negeri Malang, Malang, Jatim, Indonesia
[2] Mechanical Engineering, Universitas Negeri Malang, Malang, Jatim, Indonesia
[3] Civil Engineering, Universitas Negeri Malang, Malang, Jatim, Indonesia
[4] Mathematics, IKIP Budi Utomo, Malang, Jatim, Indonesia
[5] Electrical Engineering and Computer Science, Shibaura Institute of Technology, Tokyo, Japan

**Abstract:** The article describes a method of energy injection based on a random fluctuated commitment incorporated with Renewable Energy Sources (RES) in the power system, which is optimized using Thunderstorm Algorithm (TA) where Takagi Method (TM) is adopted for a hybrid power flow model. The RES has become one of the keys to the sustainable potential energy under environmental penetration as determining in these works to reach an operating efficiency on a power flow study. The studies are subjected to evaluate the grid performances under solar and wind energy penetration in these works. The results indicate that RES affects the efficiency of the system. TM can be applied to the hybrid structure, while TA can search for the generated power combination. TA also has opportunities for the optimum power portion to be carried out as similar as TM is helpful to the power flow. The optimal power production feeds the load demand in 1,045.1 MVA, 648.9 MW, and 361,9 MVar, where the optimal power balance covers all possibility portions for the power producers. Moreover, the five scenarios covered conventional generators and wind turbine generators, whereas local loads consume the photovoltaic power production by delivering to the load centers.
**Keywords:** Grid Performance, Power System, Renewable Energy, Solar Power, Windfarm.

# 基於風能和太陽能農場的子電廠注入電網

**摘要：**本文介紹了一種基於隨機波動承諾並結合了電力系統中可再生能源（RES）的能量注入方法，該方法使用雷暴算法（TA）進行了優化，其中 Takagi 方法（TM）用於混合潮流模型。 RES 已成為在環境滲透下實現可持續潛在能源的關鍵之一，因為在這些工作中確定要在潮流研究中達到運行效率。這些研究將評估這些工作中太陽能和風能滲透下的電網性能。結果表明，RES 影響了系統的效率。 TM 可以應用於混合結構，而 TA 可以搜索生成的功率組合。 TA 也有機會執行最佳功率部分，就像 TM 對功率流有幫助一樣。最佳發電量滿足 1,045.1 MVA，648.9 MW 和 361.9 MVar 的負載需求，其中最佳發電平衡涵蓋了發電者的所有可能部分。此外，這五個方案涵蓋了常規發電機和風力渦輪發電機，而本地負載則通過傳遞到負載中心來消耗光伏發電。
**关键词：**電網性能，電力系統，可再生能源，太陽能，風電場。

## 1. Introduction

Nowadays, a power system (PS) interconnection moves to intelligent networks covered loads and power plants. Technically, this network consists of several parts and sections used to connect large-distance load centers and even installed systems over decades where the PS is divided into many operational areas [1]. Moreover, each site has a local power grid system

Received: 8 February 2021 / Revised: 9 March 2021 / Accepted: 15 March 2021 / Published: 30 April 2021

Fund Project: The PNBP Research Grant Universitas Negeri Malang, Indonesia

About the authors: A.N. Afandi, Irham Fadlika, Langlang Gumilar, Aji P. Wibawa, Aripriharta, Syaad Patmantara, Ilham Aez, Electrical Engineering, Universitas Negeri Malang, Malang, Jatim, Indonesia; Eddy Sutadji, Mechanical Engineering, Universitas Negeri Malang, Malang, Jatim, Indonesia; Tri Kuncoro, Civil Engineering, Universitas Negeri Malang, Malang, Jatim, Indonesia; Marji, Mechanical Engineering, Universitas Negeri Malang, Malang, Jatim, Indonesia; Yunis Sulistyorini, Mathematics, IKIP Budi Utomo, Malang, Jatim, Indonesia; Goro Fujita, Electrical Engineering and Computer Science, Shibaura Institute of Technology, Tokyo, Japan

Corresponding author A.N. Afandi, an.afandi@um.ac.id

(LPGS) which is existed for covering all generating units and load demands. In contrast, the cascaded system provides high-quality services in an interconnected power grid system (IPGS). Several local grids are linked together to become an enormous IPGS topology used to network partial structures and physical sections [2].

By considering the integrated network, the PS due to subsections in terms of operating sections such as generating sites, power lines, and utilization systems [2]–[4]. The sub-systems are used to exist energy users as the final load that consumes the power for various appliances [5].

The PS is also planned to improve safety to provide high-quality energy sales to meet the rise in power demand [6]–[9]. The most critical aspects of the operation deal with the power system severity presented in the generator outage condition for defining regular operation under technical limitation, while faulted performances also consider the possible disturbance [10]–[12]. The power system performance (PSP) is used to assess the availability parameters like measured voltage drops, imbalances, or harmonic measuring power levels. The PSP is evaluated with a Power Flow Method (PFM) to determine the system's operating status by recognizing these conditions. Furthermore, the load demand grows with the power and networkability of the PS, while exploring potential primary energy sources as a renewable energy source (RES) is also being used in non-fossil fuels. The RES usages are dependent on applied current technologies for power production [13]–[16]. This paper presents the PSP considered an injection power source of the RES. The new injection method is used to control an energy transfer. These studies are also subjected to evaluate the grid performances under solar and wind energy penetration. In these works, the Thunderstorm Algorithm (TA) is applied to the system, while the Takagi method (TM) is combined for a hybrid structure of the power flow model. As many reported works that TM is helpful for the PFM. In these works, TA as a new algorithm is introduced to optimize the optimal energy producer composition.

## 2. Power Grid Development

The evaluation is used in this work to know the operational condition according to all demands. Many PFM techniques have been proposed and used for the PS, whereas Newton-Raphson and Fast Decouple are popular approaches [17], [18]. Technically, the PFM is applied to a power flow study (PFS). This analysis provides a balanced steady-state operation of the PS. Every PS bus is classified into three types of cargo and generator bus, and swing bus. The PFS is combined with the Taakagi Method and Thunderstorm Algorithm (TA) (TM). The TA structures and intelligent agents in previous works have been thoroughly discussed, while the TM for PFS is also clearly documented in [15], [19]–[21].

The PS-based fossil fuel has recently met environmental requirements, and the growing demand for security, reliability, and quality is also met. Moreover, the current commercially available power storage systems for bulk energy storage under the RES are technically and economically impossible [13]. Declining traditional fossil fuels, together with restrictions on carbon emissions and environmental policies, are the key to reducing fossil fuel combustion [15], [20]–[23]. In terms of production, demand management, network, and reserve, the effects of unit changes on renewable sources are more flexible.

In general, sectioned areas of the PS are integrated to become an interconnected network as the LPGS for delivering electricity from producers to consumers [7], [24]–[26]. Power stations may be located near an energy source. Recently, a distributed power plant can be installed closely at the load center [4], [14], [25, p.]

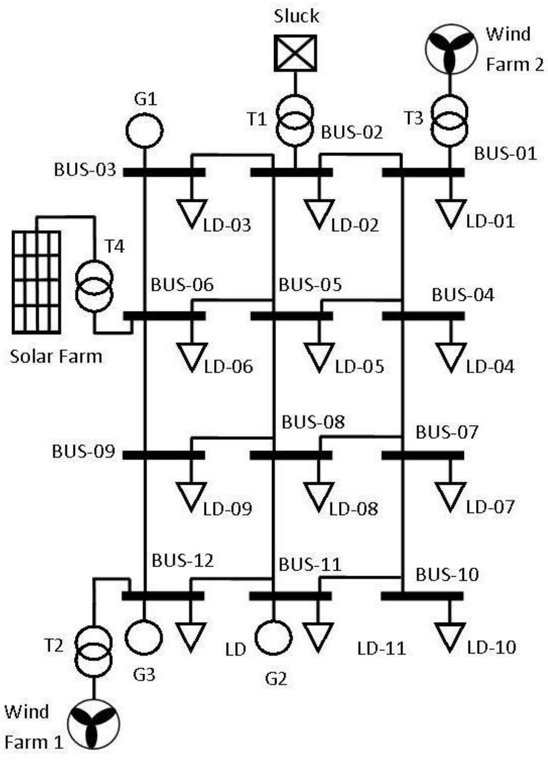


Fig.1 Grid topology interconnection

Including the RES in the PS, expansion ensures a reduction in future dependence on fossil fuels. Potential sources, like solar and wind energy, are the most popular of the RES [25], [27], [28]. Solar energy is integrated with these studies into the LPGS wind energy, as shown in Figure 1. The development of LPGS in solar energy and wind power centers is shown in Figure 1. This growth is significant for the growth of demand over the current period. This setup also increases energy supply and system capacity by installing the RES [22], [29]–[31]. According to Figure 1, this system is also expanded to the hybrid system covered for the RES at north, west, and south areas.

## 3. Evaluation Scenarios

In these works, Figure 1 is a reference for developing electricity system analysis and optimizing categories which are divided into five schemes for the LPGS. According to Figure 2, method procedures cover Entry Data, System Configuration, Load Flow Process, Optimization. Entry Data is used to put all parameters of the component used in the whole process. System Configuration is also used to select a scenario under a system configuration based on all possible conditions for the power grid operation. To perform initial, progressing, and final conditions related to all designs, the Load Flow Process is applied to the system configuration for determining current operating status. Moreover, Optimization is used to define the optimal combination based on the energy injection associated with wind and solar energy farms.

In these works, the LPGS is developed for the existing system prepared for the double voltage incoming covered for 20 kV and 70 kV. Both voltage levels are connected from different lines. These studies also take an assumption for the natural condition in constant for wind speed and solar radiation. Moreover, the connected load is presented as designed demand in Table 1. In addition, the scenarios are shown in the standard operating system integration (NOSI), captive power plant integration (CPPI), north wind farm integration (NWFI), south wind farm integration (SWFI), and solar power center integration (SPCI).

Technically, the NOSI presents the system with a normal condition before developing to the advanced design as the first condition. The CPPI covers the NOSI and an additional power plant conventional based. The NWFI consists of the NOSI, CPPI, and wind farm center in the northern area. The SWFI includes the NOSI, CPPI, NWFI, and wind farm center in the southern region. All integrated system is covered in the SPCI. In these studies, the evaluation considers Figure 1, Table 1 to Table 6. Refer to this topology of the LPGS. The PFS is subjected to determine the optimal performances based on the NOSI, CPPI, NWFI, SWFI, and SPCI.

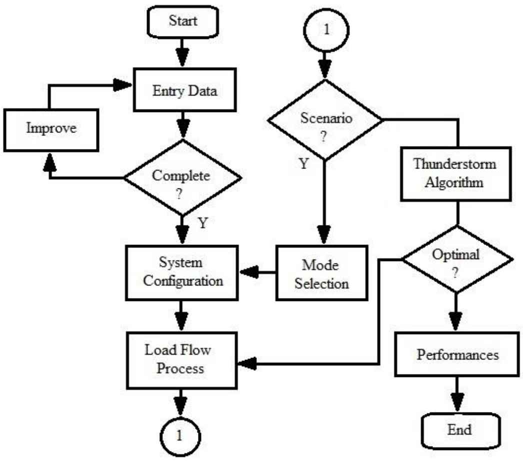


Fig. 2. Method procedures of the power grid evaluation

Table 1 Individual load conditions

| Bus | Voltage (kV) | Capacity (Kva) | (kW) | (kvar) |
|---|---|---|---|---|
| BUS-01 | 20.0 | 94,475.0 | 68,675.0 | 29,503.0 |
| BUS-02 | 20.0 | 132,963.0 | 118,465.0 | 57,810.0 |
| BUS-03 | 20.0 | 133,030.0 | 66,565.0 | 48,659.0 |
| BUS-04 | 20.0 | 82,754.0 | 43,542.0 | 22,955.0 |
| BUS-05 | 20.0 | 18,200.0 | 10,569.0 | 4,403.0 |
| BUS-06 | 20.0 | 119,927.0 | 54,740.0 | 38,251.0 |
| BUS-07 | 20.0 | 32,696.0 | 15,401.0 | 6,672.0 |
| BUS-08 | 20.0 | 129,711.0 | 63,652.0 | 33,207.0 |
| BUS-09 | 20.0 | 67,936.0 | 44,843.0 | 26,131.0 |
| BUS-10 | 20.0 | 95,355.0 | 46,223.0 | 20,023.0 |
| BUS-11 | 20.0 | 67,649.0 | 57,400.0 | 35,799.0 |
| BUS-12 | 20.0 | 70,367.0 | 58,897.0 | 38,505.0 |

Table 2 Conventional power and grid sources

| Bus | Rating (MVA) | (MW) | Eff (%) |
|---|---|---|---|
| BUS-03 | 352.9 | 300.0 | 85 |
| BUS-11 | 411.8 | 350.0 | 85 |
| BUS-12 | 588.2 | 500.0 | 85 |

Table 3 Southern wind turbine farm

| Conn1 | Rating Power (MW) | Voltage (kV) | PF (%) | Pole | Rpm |
|---|---|---|---|---|---|
| Bus-W1 | 0.225 | 0.6 | 85 | 2 | 1500 |
| Bus-W2 | 0.225 | 0.6 | 85 | 2 | 1500 |
| Bus-W3 | 0.600 | 0.6 | 85 | 2 | 1500 |
| Bus-W4 | 0.600 | 0.6 | 85 | 2 | 1500 |

Table 4 Northern wind turbine farm

| Conn2 | Rating Power (MW) | Voltage (kV) | PF (%) | Pole | Rpm |
|---|---|---|---|---|---|
| Bus-W5 | 0.225 | 0.6 | 85 | 2 | 1500 |
| Bus-W6 | 0.225 | 0.6 | 85 | 2 | 1500 |
| Bus-W7 | 0.225 | 0.6 | 85 | 2 | 1500 |
| Bus-W8 | 0.225 | 0.6 | 85 | 2 | 1500 |

Table 5 Solar power center

| Conn3 | Formation Panel (W) | Array | DC output V | kW | AC output kV | kVA |
|---|---|---|---|---|---|---|
| PVA1 | 214.5 | 4x4 | 120 | 0.3 | 0.2 | 0.3 |
| PVA2 | 214.5 | 4x4 | 120 | 0.3 | 0.2 | 0.3 |
| PVA3 | 214.5 | 4x4 | 120 | 0.3 | 0.2 | 0.3 |
| PVA4 | 214.5 | 4x4 | 120 | 0.3 | 0.2 | 0.3 |
| PVA5 | 214.5 | 4x4 | 120 | 0.3 | 0.2 | 0.3 |
| PVA6 | 214.5 | 4x4 | 120 | 0.3 | 0.2 | 0.3 |

Table 6 Interbus transformer

| Trafo | Connection From | To | Voltage (kV) | Power (MVA) |
|---|---|---|---|---|
| 1 | Bus-Sluck | BUS-02 | 70 / 20 kV | 5000 |
| 2 | Bus7 | BUS-12 | 0.6 / 20 kV | 250 |
| 3 | Bus12 | BUS-01 | 0.6 / 20 kV | 300 |
| 4 | BUS-06 | Conn3 | 20 / 0.22 kV | 100 |

In these works, the TM is used throughout the PFS to cover the PSP as detailed in [19]. The technical limitations of the PFS are restricted. In 5% of voltage violations, the appropriate operation is desired. 95 percent of power transmission is confronted with the power delivery on the power lines. TA refers to detailed processes and hierarchies in these works [15], [21], [22]. TA is inspired by a natural mechanism that is presented in several stages and procedures. These mechanisms mimic the natural phenomena influenced by cloud conditions and potential factors for developing the striking line and streaming path. The TA search mechanism for selecting solutions is used to strike processes and channel avalanches to release the population of charges.

TA also comprises different distances used for controlling the position of striking objectives associated with a hazardous factor (hf). TA sequencing is usually given as pseudo-codes [15], [20]. On this basis, TA is performed in one avalanche, 50 cloud load, 100 stream flows, 4 hazardous, and 200 clouds. Based on these principles. In addition, the achievements of TA and TM in these studies are not detailed, whereas the work is used to investigate PSP.

# 4. Grid Performance

As mentioned before that these works have been designed based on technical requirements such as 5% of voltage violations, the appropriate operation is desired. 95 percent of power transmission is confronted with the power delivery on the power lines. TA also comprises 50 cloud loads, 100 stream flows, 4 hazardous, and 200 clouds.

In this section, these works are addressed to evaluate the performances of the LPGS considered the RES based on the NOSI, CPPI, NWFI, SWFI, and SPCI. By considering these scenarios, the optimal power production feeds the load demand in 1,045.1 MVA, 648.9 MW, and 361,9 MVar as detailed in Table 1 for the individual load conditions. The optimal power balance covers all possibility portions for the power producers as given in Table 2, Table 3, Table 4, and Table 5. In these studies, the system covers transformers as listed in Table 6.

Table 8 shows the bus loading condition for all buses considered individually connected loads, while the PSP is summarized in Table 7. According to Table 8, BUS-02 is penetrated by the highest load in 14,926 A associated with the NOSI. This condition is also worked for other scenarios for the CPPI, NWFI, SWFI, and SPCI. Moreover, the lowest result is BUS-07 of the NOSI contrasted to the CPPI. In addition, another one is BUS-W8, covered in NWSI, SWFI, and SPCI. In detail, all results of the power balance are provided in Table 9 and Table 10, while the individual voltage condition is illustrated in Figure 3.

Table 7 Summary evaluation

| Status | NOSI | CPPI | NWFI | SWFI | SPCI |
|---|---|---|---|---|---|
| Buses | 13 | 13 | 18 | 23 | 24 |
| Branches | 18 | 18 | 23 | 28 | 29 |
| Generators | 2 | 3 | 3 | 3 | 3 |
| Power Grids | 1 | 1 | 1 | 1 | 1 |
| Load numbers | 12 | 12 | 12 | 12 | 12 |
| Load (MW) | 774.4 | 817.1 | 817.1 | 817.1 | 817.1 |
| Load (Mvar) | 403.2 | 443.6 | 443.7 | 443.7 | 443.7 |
| Gen (MW) | 774.4 | 817.1 | 817.1 | 817.1 | 817.1 |
| Gen (Mvar) | 403.2 | 443.6 | 443.7 | 443.7 | 443.7 |
| Loss-MW | 125.4 | 86.3 | 86.1 | 86.2 | 86.2 |
| Loss-Mvar | 41.2 | 25.8 | 25.7 | 25.8 | 25.8 |

Table 8 Bus loading condition

| Bus | Current loading bus (A) | | | | |
|---|---|---|---|---|---|
| | NOSI | CPPI | NWFI | SWFI | SPCI |
| BUS-01 | 2,471 | 2,463 | 2,467 | 2,467 | 2,467 |
| BUS-02 | 14,926 | 9,287 | 9,265 | 9,265 | 9,265 |
| BUS-03 | 4,993 | 7,832 | 7,832 | 7,832 | 7,832 |
| BUS-04 | 1,951 | 2,092 | 2,092 | 2,092 | 2,092 |
| BUS-05 | 3,663 | 3,695 | 3,695 | 3,695 | 3,695 |
| BUS-06 | 2,583 | 3,927 | 3,927 | 3,927 | 3,927 |
| BUS-07 | 676 | 689 | 689 | 689 | 689 |
| Conn1 | - | - | - | 1,576 | 1,576 |
| BUS-08 | 3,027 | 3,178 | 3,178 | 3,178 | 3,178 |
| BUS-09 | 3,195 | 2,971 | 2,971 | 2,971 | 2,971 |
| BUS-10 | 2,324 | 2,243 | 2,243 | 2,243 | 2,243 |
| BUS-11 | 5,071 | 4,925 | 4,924 | 4,924 | 4,924 |
| BUS-12 | 5,220 | 4,957 | 4,957 | 4,962 | 4,962 |
| Conn3 | | | | | 52 |
| Bus-Sluck | 4,265 | 2,631 | 2,624 | 2,624 | 2,624 |
| Bus-W1 | - | - | - | 1,576 | 1,576 |
| Bus-W2 | - | - | - | 1,384 | 1,384 |
| Bus-W3 | - | - | - | 1,181 | 1,181 |
| Bus-W4 | - | - | - | 664 | 664 |
| Bus-W5 | - | - | 948 | 948 | 948 |
| Bus-W6 | - | - | 707 | 707 | 707 |
| Bus-W7 | - | - | 468 | 468 | 468 |
| Bus-W8 | - | - | 233 | 233 | 233 |
| Conn2 | - | - | 948 | 948 | 948 |

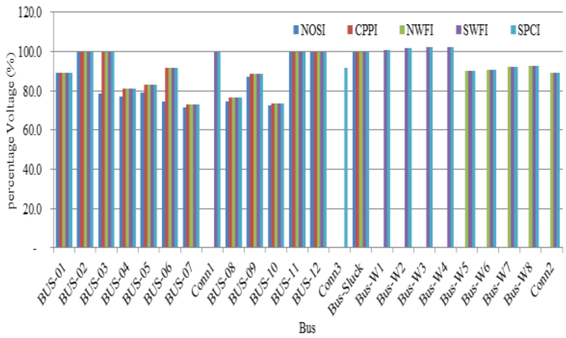


Fig. 3 Bus voltage condition

Table 9 Active Power Balance Production

| Source | Active power production (MW) | | | | |
|---|---|---|---|---|---|
| | NOSI | CPPI | NWFI | SWFI | SPCI |
| G1 | - | 227.8 | 227.8 | 227.8 | 227.8 |
| G2 | 160.6 | 155.4 | 155.4 | 155.4 | 155.4 |
| G3 | 157.0 | 148.0 | 148.0 | 146.4 | 146.4 |
| Sluck Source | 456.8 | 285.8 | 284.9 | 284.9 | 284.9 |
| WTG1 | - | - | - | 0.2 | 0.2 |
| WTG2 | - | - | - | 0.2 | 0.2 |
| WTG3 | - | - | - | 0.6 | 0.6 |
| WTG4 | - | - | - | 0.6 | 0.6 |
| WTG5 | - | - | 0.2 | 0.2 | 0.2 |
| WTG6 | - | - | 0.2 | 0.2 | 0.2 |
| WTG7 | - | - | 0.2 | 0.2 | 0.2 |
| WTG8 | - | - | 0.2 | 0.2 | 0.2 |

Table 10 Reactive power balance production

| Source | NOSI | CPPI | NWFI | SWFI |
|---|---|---|---|---|
| G1 | | 144.6 | 144.6 | 144.6 |
| G2 | 71.2 | 70.3 | 70.3 | 70.3 |
| G3 | 89.7 | 87.1 | 87.1 | 87.4 |
| Sluck Source | 242.2 | 141.7 | 141.7 | 141.7 |
| WTG1 | - | - | - | - |
| WTG2 | - | - | - | 0.1 |
| WTG3 | - | - | - | - |
| WTG4 | - | - | - | -0.4 |
| WTG5 | - | - | - | - |
| WTG6 | - | - | - | - |
| WTG7 | - | - | - | - |
| WTG8 | - | - | - | - |

Table 11 Individual active power transaction

| Power transaction | | | Power delivery (kW) | |
|---|---|---|---|---|
| Route | From | To | NOSI | CPPI |
| 1 | Bus-W4 | Bus-W3 | - | - |
| 2 | Bus-W3 | Bus-W2 | - | - |
| 3 | Bus-W2 | Bus-W1 | - | - |
| 4 | Bus-W1 | Conn1 | - | - |
| 5 | Bus-W8 | Bus-W7 | - | - |
| 6 | Bus-W7 | Bus-W6 | - | - |
| 7 | Bus-W6 | Bus-W5 | - | - |
| 8 | Bus-W5 | Conn2 | - | - |
| 9 | BUS-06 | BUS-09 | 4,389.0 | 1,153.0 |
| 10 | BUS-03 | BUS-06 | 45,010.0 | 117,360.0 |
| 11 | BUS-02 | BUS-05 | 112,555.0 | 91,293.0 |
| 12 | BUS-01 | BUS-04 | 1,377.0 | 956.0 |
| 13 | BUS-04 | BUS-07 | 2,773.0 | 4,257.0 |
| 14 | BUS-05 | BUS-08 | 21,162.0 | 30,950.0 |
| 15 | BUS-09 | BUS-12 | 98,119.0 | 89,120.0 |
| 16 | BUS-08 | BUS-11 | 28,033.0 | 25,664.0 |
| 17 | BUS-07 | BUS-10 | 7,251.0 | 4,711.0 |
| 18 | BUS-02 | BUS-03 | 146,810.0 | 3,088.0 |
| 19 | BUS-01 | BUS-02 | 78,684.0 | 78,534.0 |
| 20 | BUS-05 | BUS-06 | 9,650.0 | 22,593.0 |
| 21 | BUS-04 | BUS-05 | 46,518.0 | 53,004.0 |
| 22 | BUS-08 | BUS-09 | 34,680.0 | 32,291.0 |
| 23 | BUS-07 | BUS-08 | 5,932.0 | 7,895.0 |
| 24 | BUS-11 | BUS-12 | - | - |
| 25 | BUS-10 | BUS-11 | 75,157.0 | 72,377.0 |
| 26 | Bus-Sluck | BUS-02 | 456,789.0 | 285,750.0 |
| 27 | Bus7 | BUS-12 | - | - |
| 28 | Bus12 | BUS-01 | - | - |
| 29 | BUS-06 | Conn3 | - | - |

Table 12 Renewable active power transaction

| Power transaction | | | Power delivery (kW) | | |
|---|---|---|---|---|---|
| Route | From | To | NWFI | SWFI | SPCI |
| 1 | Bus-W4 | Bus-W3 | - | 600.0 | 600.0 |
| 2 | Bus-W3 | Bus-W2 | - | 1,196.0 | 1,196.0 |
| 3 | Bus-W2 | Bus-W1 | - | 1,409.0 | 1,409.0 |
| 4 | Bus-W1 | Conn1 | - | 1,623.0 | 1,623.0 |
| 5 | Bus-W8 | Bus-W7 | 225.0 | 225.0 | 225.0 |
| 6 | Bus-W7 | Bus-W6 | 448.0 | 448.0 | 448.0 |
| 7 | Bus-W6 | Bus-W5 | 666.0 | 666.0 | 666.0 |
| 8 | Bus-W5 | Conn2 | 886.0 | 886.0 | 886.0 |
| 9 | BUS-06 | BUS-09 | 1,153.0 | 1,153.0 | 1,154.0 |
| 10 | BUS-03 | BUS-06 | 117,357 | 117,357 | 117,341 |
| 11 | BUS-02 | BUS-05 | 91,288 | 91,288.0 | 91,287.0 |
| 12 | BUS-01 | BUS-04 | 968.0 | 968.0 | 968.0 |
| 13 | BUS-04 | BUS-07 | 4,258.0 | 4,258.0 | 4,258.0 |
| 14 | BUS-05 | BUS-08 | 30,953.0 | 30,953.0 | 30,953.0 |
| 15 | BUS-09 | BUS-12 | 89,119.0 | 89,119.0 | 89,119.0 |
| 16 | BUS-08 | BUS-11 | 25,663.0 | 25,663.0 | 25,663.0 |
| 17 | BUS-07 | BUS-10 | 4,710.0 | 4,710.0 | 4,710.0 |
| 18 | BUS-02 | BUS-03 | 3,084.0 | 3,084.0 | 3,084.0 |
| 19 | BUS-01 | BUS-02 | 77,667.0 | 77,667.0 | 77,667.0 |
| 20 | BUS-05 | BUS-06 | 22,590.0 | 22,590.0 | 22,593.0 |
| 21 | BUS-04 | BUS-05 | 52,995.0 | 52,995.0 | 52,995.0 |
| 22 | BUS-08 | BUS-09 | 32,289.0 | 32,289.0 | 32,289.0 |
| 23 | BUS-07 | BUS-08 | 7,896.0 | 7,896.0 | 7,896.0 |
| 24 | BUS-11 | BUS-12 | - | - | - |
| 25 | BUS-10 | BUS-11 | 72,376.0 | 72,376.0 | 72,376.0 |
| 26 | Bus-Sluck | BUS-02 | 284,882 | 284,882 | 284,880 |
| 27 | Bus7 | BUS-12 | - | 1,602.0 | 1,602.0 |
| 28 | Bus12 | BUS-01 | 879.0 | 879.0 | 879.0 |
| 29 | BUS-06 | Conn3 | - | - | 18.3 |

Table 13 Reactive power transaction

| Route | From | To | NOSI | CPPI | NWFI | SWFI |
|---|---|---|---|---|---|---|
| 1 | Bus-W4 | Bus-W3 | - | - | - | -372.0 |
| 2 | Bus-W3 | Bus-W2 | - | - | - | -377.0 |
| 3 | Bus-W2 | Bus-W1 | - | - | - | -292.0 |
| 4 | Bus-W1 | Conn1 | - | - | - | -313.0 |
| 5 | Bus-W8 | Bus-W7 | - | - | - | - |
| 6 | Bus-W7 | Bus-W6 | - | - | -0.6 | -0.6 |
| 7 | Bus-W6 | Bus-W5 | - | - | -3.2 | -3.2 |
| 8 | Bus-W5 | Conn2 | - | - | -8.8 | -8.8 |
| 9 | BUS-06 | BUS-09 | 795.0 | 654.0 | 654.0 | 654.0 |
| 10 | BUS-03 | BUS-06 | 29,392 | 68,808 | 68,811 | 68,811.0 |
| 11 | BUS-02 | BUS-05 | 57,380 | 46,543 | 46,542 | 46,542.0 |
| 12 | BUS-01 | BUS-04 | 328.0 | 253.0 | 250.0 | 250.0 |
| 13 | BUS-04 | BUS-07 | 978.0 | 1,376.0 | 1,376.0 | 1,376.0 |
| 14 | BUS-05 | BUS-08 | 11,349 | 15,431 | 15,429 | 15,429.0 |
| 15 | BUS-09 | BUS-12 | 51,212 | 48,544 | 48,545 | 48,545.0 |
| 16 | BUS-08 | BUS-11 | 6,546.0 | 6,267 | 6,267.0 | 6,267.0 |
| 17 | BUS-07 | BUS-10 | 3,760.0 | 2,923 | 2,924.0 | 2,924.0 |
| 18 | BUS-02 | BUS-03 | 90,017 | -2,701 | -2,691.0 | -2,691.0 |
| 19 | BUS-01 | BUS-02 | 32,762 | 32,809 | 32,838 | 32,838.0 |
| 20 | BUS-05 | BUS-06 | 9,198.0 | 6,654.0 | 6,657.0 | 6,657.0 |
| 21 | BUS-04 | BUS-05 | 24,076 | 26,971 | 26,974 | 26,974.0 |
| 22 | BUS-08 | BUS-09 | 21,213 | 19,818 | 19,819 | 19,819.0 |
| 23 | BUS-07 | BUS-08 | 2,032.0 | 2,755.0 | 2,755.0 | 2,755.0 |
| 24 | BUS-11 | BUS-12 | - | - | - | - |
| 25 | BUS-10 | BUS-11 | 28,857 | 28,211 | 28,212 | 28,212.0 |
| 26 | Bus-Sluck | BUS-02 | 242,239 | 141,700 | 141,710 | 141,710 |
| 27 | Bus7 | BUS-12 | - | - | - | -342.0 |
| 28 | Bus12 | BUS-01 | - | - | -18.9 | -18.9 |
| 29 | BUS-06 | Conn3 | - | - | - | - |

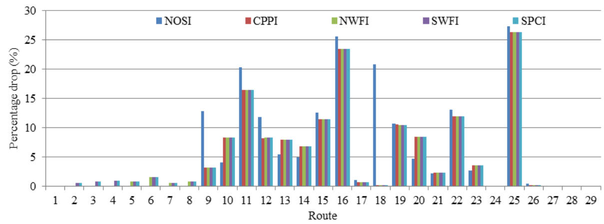


Fig. 4 The percentage voltage drop of the power transaction

As given in Table 9 and Table 10, the power production is balanced for the active and reactive power portions. This table illustrates all conditions for the five scenarios covered for conventional generators and wind turbine generators, whereas local loads consume the photovoltaic power production. In detail, the power transactions are detailed in Table 11, Table 12, and Table 13 for the power delivery to the load centers. At the same time, the system performances for individual voltage drops are depicted in Figure 4.

## 5. Conclusion

This paper analyzes the local energy grid system considering the solar and wind energy sources (RES). The evaluation is examined by Takaguchi Method (TM) and Thunderstorm Algorithm in power flow (TA). These works show that the RES penetrates power generation and affects the performance of the system. TM and TA can apply to the assessment of power flow. For future work, it is recommended to implement the actual application to the power grid and to disclose computer structures based on various parameters of TM-TA.

## References

[1] AFANDI A. N., WIBAWA A.P., PADMANTARA S. Designed operating approach of economic dispatch for Java Bali power grid areas considered wind energy and pollutant emission optimized using thunderstorm algorithm based on forward cloud charge mechanism. *The International Review of Electrical Engineering (IREE)*, 2018, 13(1): 59-68. DOI: 10.15866/iree.v13i1.14687.

[2] CUFFE P. and KEANE A. Visualizing the electrical structure of power systems. *IEEE Systems Journal*, 2017, 11(3): 1810–1821. DOI: 10.1109/JSYST.2015.2427994.

[3] BO Z. Q., LIN X. N., WANG Q. P. et al. Developments of power system protection and control. *Protection and Control of Modern Power Systems*, 2016, 1(1): 7. DOI: 10.1186/s41601-016-0012-2.

[4] TUTKUN N., CAN O., and AFANDI A. N. Low-cost operation of an off-grid wind-PV system is electrifying residential homes through combinatorial optimization by the RCGA. In: *2017 5th International Conference on Electrical, Electronics and Information Engineering (ICEEIE), Malang, Indonesia, October 6-8, 2017.* Yogyakarta: IEEE, 2017: 38–42. DOI: 10.1109/ICEEIE.2017.8328759.

[5] AFANDI A. N., FADLIKA I., and SULISTYORINI Y. Solution of dynamic economic dispatch considered dynamic penalty factor. In: *2016 3rd Conference on Power Engineering and Renewable Energy (ICPERE), Yogyakarta, Indonesia, November 29-30, 2016.* Yogyakarta: IEEE, 2016: 241–246. DOI: 10.1109/ICPERE.2016.7904870.

[6] DEBNATH R., KUMAR D., and MOHANTA D. K., Effective demand side management (DSM) strategies for the deregulated market environments. In: *2017 Conference on Emerging Devices and Smart Systems (ICEDSS), Mahendhirapuri, India, March 3-4, 2017.* New Delhi: IEEE, 2016: 110–115. DOI: 10.1109/ICEDSS.2017.8073668.

[7] GAMMON R. J. L., BOAIT P. J., and ADVANI V., Management of demand profiles on mini-grids in developing countries using timeslot allocation. In: *2016 IEEE PES PowerAfrica, Livingstone, June 2-5, 2016.* Pretoria: IEEE, 2016: 41–45. DOI: 10.1109/PowerAfrica.2016.7556566.

[8] AFANDI A. N. Solving combined economic and emission dispatch using harvest season artificial bee colony algorithm considering food source placements and modified rates. *International Journal on Electrical Engineering and Informatics,* 2014, 6: 267.

[9] AFANDI A. N., SULISTYORINI Y., MIYAUCHI H., et al. The penetration of pollutant productions on dynamic generated power operations optimized using a novel evolutionary algorithm. *International Journal on Advanced Science, Engineering and Information Technology,* 2017, 7(5): 1825–1831. DOI: 10.18517/ijaseit.7.5.1635.

[10] LAMMERT G., BOEMER J., PREMM D., et al. Impact of fault ride-through and dynamic reactive power support of photovoltaic systems on short-term voltage stability, In: *2017 IEEE Manchester PowerTech,* Manchester, *UK, June 18-22, 2017.* Piscataway, NJ: IEEE, 2017: 1–6. doi: 10.1109/PTC.2017.7980926.

[11] LIU Z. and ZHANG Z. Quantifying transient stability of generators by basin stability and Kuramoto-like models. In: *2017 North American Power Symposium (NAPS), Morgantown, West Virginia, September 17-19, 2017.* Piscataway, NJ: IEEE, 2017: 1–6. DOI: 10.1109/NAPS.2017.8107260.

[12] SENGUPTA A. and KACHAVE D. Spatial and temporal redundancy for transient fault-tolerant datapath. *IEEE Transactions on Aerospace and Electronic Systems,* 2017, 99: 1-11. DOI: 10.1109/TAES.2017.2776038.

[13] GANAPATHY A., SOMAN G., VM G. M. et al. Online energy audit and renewable energy management system. In: 2*016 International Conference on Computing Communication Control and Automation (ICCUBEA)*, Pune, *India, August 12-13, 2016*. Piscataway, NJ: IEEE, 2016: 61–66. DOI: 10.1109/ICCUBEA.2016.7860035.

[14] MENCHAFOU Y., MARKHI H. E., ZAHRI M. Impact of distributed generation integration in electric power distribution systems on fault location methods. In: *2015 3rd International Renewable and Sustainable Energy Conference (IRSEC), Marrakech, Ouarzazate, Morocco, December 10–13, 201*5. 2015: 1–5. DOI: 10.1109/IRSEC.2015.7455137.

[15] AFANDI A. N. Thunderstorm algorithm for assessing thermal power plants of the integrated power system operation with an environmental requirement. *International Journal of Engineering and Technology,* 2016, 8: 1102–1111.

[16] AFANDI A. N. Optimal scheduling power generations using HSABC algorithm considered a new penalty factor approach. In: *The 2nd IEEE Conference on Power Engineering and Renewable Energy (ICPERE) 2014*. Piscataway, NJ: IEEE, 2014: 13–18. DOI: 10.1109/ICPERE.2014.7067227.

[17] CHATTERJEE S. and MANDAL S. A novel comparison of Gauss-Seidel and Newton- Raphson methods for load flow analysis. In: *2017 International Conference on Power and Embedded Drive Control (ICPEDC), Chennai, India, March 16-18, 2017*. Piscataway, NJ: IEEE, 2017: 1–7, DOI: 10.1109/ICPEDC.2017.8081050.

[18] DENG J.-J. and CHIANG H.-D. Convergence region of Newton Iterative Power Flow Method: Numerical studies. *Journal of Applied Mathematics*, 2013: 509496. DOI: 10.1155/2013/509496.

[19] HASANIEN H. M. and MUYEEN S. M. A Taguchi approach for optimum design of proportional-integral controllers in the cascaded control scheme. *IEEE Transactions on Power Systems*, 2013, 28: 1636–1644. doi: 10.1109/tpwrs.2012.2224385.

[20] AFANDI A. N. and SULISTYORINI Y., Thunderstorm algorithm for determining unit commitment in power system operation. *Journal of Engineering and Technological Sciences*, 2016: 48(6): 743–752. DOI: 10.5614/j.eng.technol.sci.2016.48.6.7.

[21] AFANDI A. N., SULISTYORINI Y., FUJITA G., et al. Renewable energy inclusion on economic power optimization using thunderstorm algorithm. In: *2017 4th International Conference on Electrical Engineering, Computer Science and Informatics (EECSI), Jogikarta, Indonesia, September 19-21, 2017.* Piscataway, NJ: IEEE, 2017: 1–6. DOI: 10.1109/EECSI.2017.8239141.

[22] AFANDI A. N., FADLIKA I., and ANDOKO A. Comparing performances of evolutionary algorithms on the emission dispatch and economic dispatch problem. In: *TELKOMNIKA (Telecommunication, Computing Electronics , and Control),* 2015, 13(4): 1187–1193. DOI: 10.12928/telkomnika.v13i4.3166.

[23] AFANDI A. N. Optimal solution of the EPED problem considering space areas of HSABC on the power system operation. *International Journal of Engineering and Technology,* 2015:7(5):1824-1830.

[24] EL-SHIMY M., MOSTAFA N., AFANDI A. N. et al. Impact of load models on grid-connected wind power plants' static and dynamic performances: A comparative analysis. *Mathematics and Computers in Simulation*, 2018, 149:91-108. DOI: 10.1016/j.matcom.2018.02.003.

[25] EL-SHIMY M., ATTIA M. A., MOSTAFA N. et al. Performance of grid-connected wind power plants as affected by load models: A comparative study. In: *2017 5th International Conference on Electrical, Electronics and Information Engineering (ICEEIE), Malang, Indonesia,*

*October 6-8, 2017*. Yogyakarta: IEEE, 2017: 1–8. DOI: 10.1109/ICEEIE.2017.8328753.
[26] AFANDI A. N. and MIYAUCHI H. Improved artificial bee colony algorithm considering harvest season for computing economic dispatch on the power system. *IEEJ Transactions on Electrical and Electronic Engineering*, 2014, 9(3): 251–257. DOI: 10.1002/tee.21963.
[27] KURIAN S., SINDHU T. K., and CHERIYAN E. P., Composite pricing strategy for energy storage in wind electric generation. In: *2015 IEEE PES Asia-Pacific Power and Energy Engineering Conference (APPEEC), Brisbane, Australia, November 15-18, 2015*. Piscataway, NJ: IEEE, 2015: 1–5. DOI: 10.1109/APPEEC.2015.7380920.
[28] LI Y., MIAO S., LUO X. et al. Optimization model for the power system scheduling with wind generation and compressed air energy storage combination. In: *2016 22nd International Conference on Automation and Computing (ICAC), Colchester, UK, on September 7-8,* 2016: 300–305. DOI: 10.1109/IConAC.2016.7604936.
[29] GUPTA N., SWARNKAR A., and NIAZI K. R., Distribution network reconfiguration for power quality and reliability improvement using genetic algorithms. *International Journal of Electrical Power & Energy Systems*, 2014, 54: 664–671. DOI: 10.1016/j.ijepes.2013.08.016.
[30] IMRAN A.M. and KOWSALYA M. A new power system reconfiguration scheme for power loss minimization and voltage profile enhancement using Fireworks Algorithm *International Journal of Electrical Power & Energy Systems*, 2014, 62:312–322. DOI: 10.1016/j.ijepes.2014.04.034.
[31] ARENGGA D., AGUSTIN W., RAHMAWATI Y. et al. SPEKTRA fast and smart software for renewable energy management. *IOP Conference Series: Earth and Environmental Science*. 2018, 105: 012077. DOI: 10.1088/1755-1315/105/1/012077.

**参考文:**

[1] AFANDI A. N.，WIBAWA A.P.，PADMANTARA S. 为巴厘岛爪哇巴厘岛电网设计的经济调度运行方法，考虑了使用基于前向云电荷机制的雷暴算法优化风能和污染物排放。国际电气工程评论（IREE），2018，13（1）：59-68。土井：10.15866 / iree.v13i1.14687。
[2] CUFFE P. 和 KEANE A。可视化电力系统的电气结构。电气工程师学会系统杂志，2017，11（3）：1810-1821。土井：10.1109 / JSYST.2015.2427994。
[3] BO Z. Q., LIN X. N., WANG Q. P.等。电力系统保护与控制的发展。现代电力系统保护与控制，2016，1（1）：7. DOI：10.1186 / s41601-016-0012-2。
[4] TUTKUN N., CAN O. 和 AFANDI A. N. 离网式风力光伏发电系统的低成本运营通过 RCGA 的组合优化使住宅房屋电气化。在：2017 年第五届电气，电子和信息工程国际会议（国际电子工程师学会），印度尼西亚玛琅，2017 年 10 月 6 日至 8 日。日惹：电气工程师学会，2017 年：38-42。土井：10.1109 / ICEEIE.2017.8328759。
[5] AFANDI A. N.，FADLIKA I. 和 SULISTYORINI Y. 考虑动态惩罚因子的动态经济调度解决方案。在：2016 年第三届电力工程与可再生能源大会（卡珀），印度尼西亚日惹，2016 年 11 月 29 日至 30 日。日惹：电气工程师学会，2016 年：241–246。土井：10.1109 / ICPERE.2016.7904870。
[6] DEBNATH R., KUMAR D. 和 MOHANTA D.K.，针对放松管制的市场环境的有效需求侧管理（帝斯曼）策略。在：2017 年新兴设备和智能系统会议（信息系统），印度马亨德拉普里，2017 年 3-4 日。新德里：电气工程师学会，2016 年：110–115。DOI：10.1109 / ICEDSS.2017.8073668。
[7] GAMMON R. J. L., BOAIT P. J. 和 ADVANI V.，使用时隙分配管理发展中国家小型电网的需求概况。在：2016 电子工程师学会电力非洲，利文斯通，2016 年 6 月 2 日至 5 日。比勒陀利亚：电气工程师学会，2016 年：41–45。DOI：10.1109/PowerAfrica.2016.7556566。
[8] AFANDI A. N. 使用收成季节的人工蜂群算法解决了经济和排放的联合调度，同时考虑了食物来源的位置和修改后的比率。国际电气工程与信息学杂志，2014，6：267。
[9] AFANDI A. N.，SULISTYORINI Y.，MIYAUCHI H. 等。使用新型进化算法优化了污染物产生对动态发电操作的渗透。国际先进科学，工程与信息技术杂志，2017，7（5）：1825-1831。DOI：10.18517/ijaseit.7.5.1635。
[10] LAMMERT G., BOEMER J., PREMMM D. 等。光伏系统的故障穿越和动态无功功率支持对短期电压稳定性的影响，in：2017 电气工程师学会曼彻斯特电力技术，曼彻斯特，英国，2017 年 6 月 18-22 日。新泽西州皮斯卡塔维：电气工程师学会，2017：1-6 。土井：10.1109 / PTC.2017.7980926。
[11]刘中和张中。用盆地稳定性和类仓本模型对发电机的暂态稳定性进行量化。在：2017 年北美电力研讨会（净资产收益率），西弗吉尼亚州摩根敦，2017 年 9 月 17 日至 19 日。新泽西州皮斯卡塔维，新泽西：IEEE，2017 年：1-6。DOI：10.1109 / NAPS.2017.8107260。
[12] SENGUPTA A. 和 KACHAVE D. 瞬时容错数据路径的空间和时间冗余。电气工程师学会航空航天和电子系统学报，2017，99：1-11。土井：10.1109 / TAES.2017.2776038。
[13] GANAPATHY A., SOMAN G., VM G. M. 等。在线能源审计和可再生能源管理系统。在：2016 年国际计算通信控制与自动化会议（古巴），印度浦那，2016 年 8 月 12 日至 13 日。皮斯卡塔维，新泽西州：电气工程师学会，2016 年：61–66。土井：10.1109 / ICCUBEA.2016.7860035。
[14] MENCHAFOU Y., MARKHI H. E., ZAHRI M. 配电系统中分布式发电集成对故障定位方法的影响。在：2015 年第三届国际可再生与可持续能源会议（IRSEC），摩洛哥，瓦尔扎扎特，马拉喀什，2015 年 12 月 10 日至 13 日。2015 年：1-5。土井：10.1109 / IRSEC.2015.7455137。
[15] AFANDI A. N. 雷暴算法，用于根据环境要求评估火力发电厂的综合电力系统运行。国际工程技术杂志，2016，8：1102-1111。

[16] AFANDI A. N. 使用汇丰银行算法的最优调度发电被认为是一种新的惩罚因子方法。于：2014 年第二届电气工程师学会电力工程与可再生能源大会（卡珀）。新泽西州皮斯卡塔维，新泽西州：电气工程师学会，2014 年：13–18。土井：10.1109 / ICPERE.2014.7067227。
[17] CHATTERJEE S. 和 MANDAL S. 一种用于潮流分析的高斯·赛德尔方法和牛顿-拉夫森方法的新颖比较。于：2017 年电源与嵌入式驱动控制国际会议（太平洋经济合作发展委员会），印度金奈，2017 年 3 月 16 日至 18 日。新泽西州皮斯卡塔维，新泽西州：电气工程师学会，2017 年：1–7，土井：10.1109 / ICPEDC.2017.8081050。
[18] 邓建强。 和 蒋 H.-D. 牛顿迭代潮流算法的收敛区域：数值研究。应用数学学报，2013：509496。土井：10.1155 / 2013/509496。
[19] HASANIEN H. M. 和 MUYEEN S. M. 一种田口方法，用于级联控制方案中比例积分控制器的最佳设计。电气工程师学会电力系统交易，2013，28：1636-1644。 doi：10.1109 / tpwrs.2012.2224385。
[20] AFANDI A. N. 和 SULISTYORINI Y.，雷暴算法，用于确定电力系统运行中的机组承诺。工程技术学报，2016：48（6）：743–752。土井：10.5614 / j.eng.technol.sci.2016.48.6.7。
[21] AFANDI A. N.，SULISTYORINI Y.，FUJITA G. 等。使用雷暴算法将可再生能源纳入经济动力优化中。在：2017 年第四届电气工程，计算机科学和信息学国际会议（电气与电子工程学会），印度尼西亚，乔吉卡塔，2017 年 9 月 19 日至 21 日。新泽西州皮斯卡塔维，电气工程师学会，2017 年：1-6。土井：10.1109/EECSI.2017.8239141。
[22] AFANDI A. N.，FADLIKA I. 和 ANDOKO A. 比较进化算法在排放调度和经济调度问题上的性能。于：TELKOMNIKA（电信，计算电子与控制），2015，13（4）：1187–1193。土井：10.12928/telkomnika.v13i4.3166。
[23] AFANDI A. N. 考虑电力系统运行中汇丰银行空间区域的聚四氟乙烯问题的最佳解决方案。国际工程技术杂志，2015：7（5）：1824-1830。
[24] EL-SHIMY M.，MOSTAFA N.，AFANDI A. N. 等。负荷模型对并网风电厂静态和动态性能的影响：比较分析。数学与模拟计算机，2018，149：91-108。DOI：10.1016 / j.matcom.2018.02.003。
[25] EL-SHIMY M.，ATTIA M.A.，MOSTAFA N. 等。受负荷模型影响的并网风力发电厂的性能：一项比较研究。在：2017 年第五届电气，电子和信息工程国际会议（国际电子工程师学会），印度尼西亚玛琅，2017 年 10 月 6 日至 8 日。日惹：电气工程师学会，2017 年：1-8。土井：10.1109 / ICEEIE.2017.8328753。
[26] AFANDI A. N. 和 MIYAUCHI H. 考虑到收获季节的改进人工蜂群算法，用于计算电力系统的经济调度。电气工程师学会电气电子工程学报，2014，9（3）：251–257。 DOI：10.1002 / tee.21963。
[27] KURIAN S.，SINDHU T. K. 和 CHERIYAN E. P.，风力发电中能量存储的综合定价策略。在：2015 年电子工程师学会亚太电力和能源工程会议（APPEEC），澳大利亚布里斯班，2015 年 11 月 15 日至 18 日。皮斯卡塔维，新泽西州：电气工程师学会，2015 年：1-5。土井：10.1109 / APPEEC.2015.7380920。
[28]李 Y，苗 S，罗 X 等。风力发电与压缩空气储能相结合的电力系统调度优化模型。在：2016 年第 22 届国际自动化与计算国际会议（廉政公署），英国科尔切斯特，2016 年 9 月 7 日至 8 日：300–305。DOI：10.1109/IConAC.2016.7604936。
[29] GUPTA N.，SWARNKAR A. 和 NIAZI K. R.，配电网重新配置，使用遗传算法提高电能质量和可靠性。国际电力与能源系统杂志，2014，54：664–671。土井：10.1016 / j.ijepes.2013.08.016。
[30] IMRAN A.M. 和 KOWSALYA M. 使用烟花算法的电力系统重新配置新方案，以最小化功率损耗并增强电压曲线国际电力与能源系统杂志，2014，62：312-322。土井：10.1016 / j.ijepes.2014.04.034。
[31] ARENGGA D.，AGUSTIN W.，RAHMAWATI Y.等。斯派克特拉快速，智能的可再生能源管理软件。眼压会议系列：地球与环境科学。2018，105：012077. 土井：10.1088/1755-1315/105/1/012077。